Enhancement of optical nonlinearity in periodic gold nanoparticle arrays

2006 Nanotechnology 17 4274

(http://iopscience.iop.org/0957-4484/17/16/045)

INSTITUTE OF PHYSICS PUBLISHING NANOTECHNOLOGY
Nanotechnology **17** (2006) 4274–4277 doi:10.1088/0957-4484/17/16/045

Enhancement of optical nonlinearity in periodic gold nanoparticle arrays

Hong Shen[1], **Bolin Cheng, Guowei Lu, Tingyin Ning, Dongyi Guan, Yueliang Zhou and Zhenghao Chen**

Beijing National Laboratory for Condensed Matter Physics, Institute of Physics, Chinese Academy of Sciences, Beijing 100080, People's Republic of China

E-mail: hongshen@aphy.iphy.ac.cn

Received 1 March 2006, in final form 11 July 2006
Published 7 August 2006
Online at stacks.iop.org/Nano/17/4274

Abstract
Linear and nonlinear optical properties of periodic triangular Au nanoparticle arrays were investigated. We compared the optical nonlinearity of periodic Au nanoparticle arrays with that of the ultra-thin gold film consisting of randomly distributed spheroidal clusters. A pronounced enhancement of the third-order nonlinear optical susceptibility $\chi^{(3)}$ in Au arrays was observed, and the figure of merit, $\chi^{(3)}/\alpha$, of the periodic nanoparticle arrays is one order of magnitude larger than that of the ultra-thin film. Such an enhancement of the optical nonlinearity could be due to the strong local field near the triangular nanoparticles.

(Some figures in this article are in colour only in the electronic version)

1. Introduction

Nonlinear optical materials, especially in the form of thin films, are of great practical importance for future applications in optical signal processing, optical limiting and nonlinear optical devices [1, 2]. Composite films comprising metal nanoclusters embedded in dielectric matrices have been widely investigated due to their large third-order susceptibility and ultra-fast response time [3–5]. However, almost all the previous investigations were limited to the systems of spheroidal metal particles randomly distributed in the dielectric matrices. Periodic metal nanoparticle arrays were fabricated in recent years, and the linear optical properties can be systematically tuned by changing the nanoparticle shape and size [6]. But the nonlinear optical properties of such nanoparticle arrays have not been investigated yet. Theoretical studies of Yuen *et al* [7] and of Huang and Yu [8] indicated that anisotropy of both the shape and geometric distribution of the metal nanoparticles could greatly enhance the optical nonlinearity $\chi^{(3)}$ as well as the figure of merit (FOM), defined as $\chi^{(3)}/\alpha$ (where α is the absorption coefficient), which is more important for practical use. The electrorheological or magnetorheological effect was suggested to induce the anisotropic microstructure in composite materials [9, 10]. Recently, Guan *et al* [11] proposed a method to induce metal–particle orientation by applying a parallel electric field during film growth, and an enhancement of the FOM in the $Ag/BaTiO_3$ composite films was observed. In this paper, nonlinear optical properties of periodic nanoparticles arrays with nonspheroidal particles have been investigated using the z-scan method [12]. As a reference, the optical nonlinearity of an ultra-thin gold film consisting of randomly distributed spheroidal clusters was also studied. The results demonstrate that the shapes of metal particles have a pronounced effect on the third-order nonlinear optical susceptibility of materials as well as the FOM.

2. Samples and experiments

The periodic gold nanoparticle arrays were fabricated using nanosphere lithography (NSL) [6], an inexpensive, simple, and high-throughout nanofabrication technique. The fabrication process began with the self-assembly of polystyrene nanospheres with diameters of 200 nm to form a single-layer colloidal nanosphere mask on the fused quartz substrates. By dropping 30 μl of nanosphere solution onto a cleaned quartz substrate, which was inclined between 4° and 6° in a chamber with saturated humidity at a temperature of 35 °C, we successfully formed an homogenous, dense nanosphere monolayer with an area larger than 1 cm^2. After the nanosphere masks were dry, the substrates were mounted

[1] Author to whom any correspondence should be addressed.

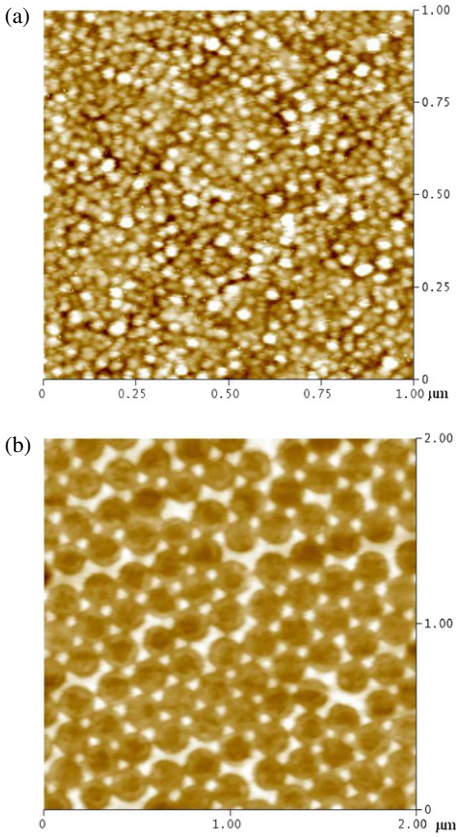

Figure 1. AFM images of the ultra-thin gold film and nanoparticle arrays: (a) N1 (film, 12 nm); (b) N3 (array, 14 nm).

into a pulsed laser deposition (PLD) system [13]. A XeCl excimer laser (308 nm, 17 ns, 2 J cm^{-2}) operating at a repetition rate of 2 Hz was focused onto a high-purity gold target mounted on a rotating holder. By varying the deposition time, gold films with different thicknesses were deposited on the substrates in vacuum (5×10^{-3} Pa) at room temperature. After the nanosphere masks were completely removed by ultrasonication in chloroform, gold nanoparticle arrays with well-ordered two-dimensional periodic structures were obtained. Additionally, ultra-thin gold film was prepared by the same PLD system on the fused quartz substrate in N_2 atmosphere at 10 Pa, with the substrate temperature maintained at 650 °C during deposition. The thickness of the gold film was measured to be 12 nm by a Dektak 8 surface stylus profiler (Veeco company).

The linear optical absorption properties were measured at room temperature from 330 to 800 nm with a Spectrapro500i spectrophotometer (Acton Research Corporation). The absorption spectrum was corrected automatically, taking into account the absorbance from the quartz substrates. The nonlinear optical properties of the ultra-thin gold film and the periodic nanoparticle arrays were investigated using z-scan technique. In our experiments, a mode-locked Nd:YAG laser with a frequency doubled at 532 nm and characterized by a pulse duration of 25 ps at a repetition rate of 1 Hz was used as the light source. The laser beam was focused onto the sample by a 120 mm focal length lens, leading to a measured beam waist (ω_0) of 30 μm, and a pulse energy of 3.7 μJ at

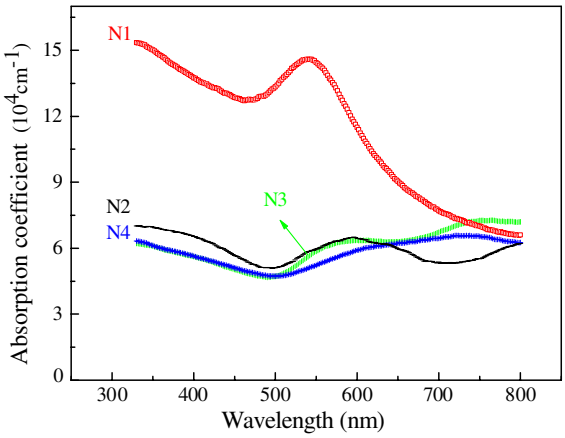

Figure 2. Optical absorption properties of the samples: (a) N1 (film, 12 nm); (b) N2 (array, 8 nm); (c) N3 (array, 14 nm); (d) N4 (array, 26 nm).

the focus. The on-axis transmitted beam energy, the reference beam energy, as well as the ratios of them, were measured using an energy ratio meter (Rm 6600, Laser Probe Corp.) simultaneously.

3. Results and discussion

The microstructures of the gold nanoparticle arrays and ultra-thin film were investigated by atomic force microscopy (AFM). Figure 1(a) gives an AFM image of a 1×1 μm^2 area of the ultra-thin gold film. As can be seen, the gold film prepared using the PLD technique at high temperature showed a clustered surface with randomly distributed spheroidal particles. The mean diameter of the spheroidal particles is about 30 nm. Figure 1(b) shows an AFM image for the gold nanoparticle array with an out-of-plane height of 14 nm. The image exhibits a hexagonal patterned two-dimensional (2D) periodic nanoparticle arrays consisting of homogenous triangular-shaped gold nanoparticles. The in-plane particle diameter, defined as the perpendicular bisector of the equilateral triangle, is estimated to be about 45 nm. The out-of-plane height of the nanoparticle arrays can be varied from 8 to 30 nm, depending on the deposition time.

For the investigations of optical properties, four samples, noted as, N1, N2, N3, and N4, were investigated. N1 is an ultra-thin gold film with a thickness of 12 nm, while samples N2, N3, and N4 are gold nanoparticle arrays with out-of-plane heights of 8, 14, and 26 nm, respectively. Figure 2 shows the optical absorption spectra of the ultra-thin gold film and nanoparticle arrays. As shown in figure 2, a strong absorption peak due to the surface plasmon resonance (SPR) of Au clusters was observed at around 545 nm for N1. Such a strong SPR peak in the absorption spectrum evidences the clustered surface of the ultra-thin gold film. In the case of nanoparticle arrays (N2–N4), the absorption was greatly reduced and SPR peaks shifted towards longer wavelengths.

Typical z-scan results for N1 and N3 are shown in figures 3 and 4, respectively. The open circles indicate the measured data, with each point corresponding to the average value of 15 measurements. The solid line represents a theoretical fit [12]. As the quartz substrate has a very weak nonlinear

Table 1. Linear and nonlinear optical properties of Au film (N1) and nanoparticle arrays (N2–N4) at a wavelength of 532 nm.

Sample no.	Thickness/height (nm)	α (10^4 cm^{-1})	Re $\chi^{(3)}$ (10^{-9} esu)	Im $\chi^{(3)}$ (10^{-9} esu)	$\chi^{(3)}$ (10^{-9} esu)	$\chi^{(3)}/\alpha$ (esu cm)
N1	12	14.4	−1.1	−1.0	1.5 ± 0.3	$(1.0 \pm 0.2) \times 10^{-14}$
N2	8	5.9	−6.1	−6.9	9.2 ± 2.3	$(1.6 \pm 0.4) \times 10^{-13}$
N3	14	5.4	−7.3	−5.1	8.9 ± 1.7	$(1.6 \pm 0.3) \times 10^{-13}$
N4	26	5.0	−6.9	−5.9	9.0 ± 1.5	$(1.8 \pm 0.3) \times 10^{-13}$

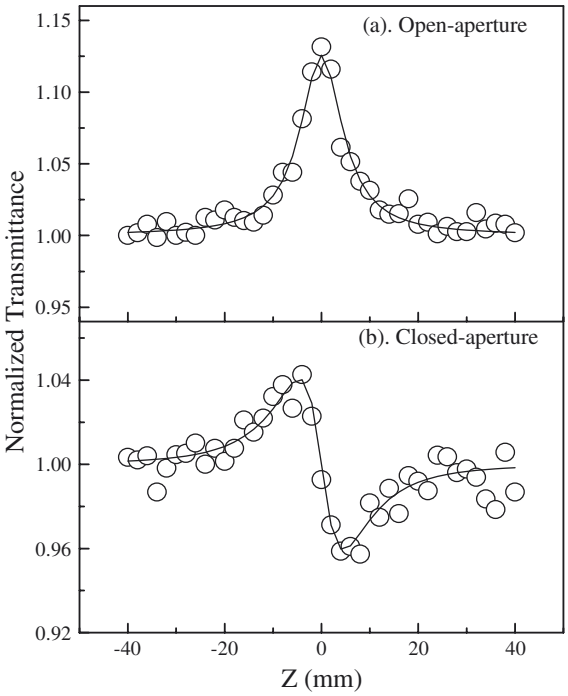

Figure 3. Z-scan results of N1 with open (a) and closed (b) aperture. The solid lines indicate the theoretical fit.

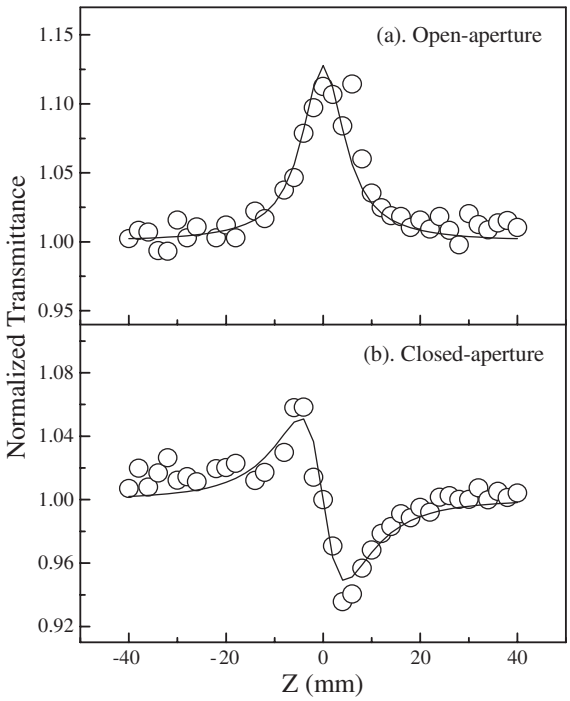

Figure 4. Z-scan results of N3 with open (a) and closed (b) aperture. The solid lines indicate the theoretical fit.

optical response, as measured by the same z-scan setup, the observed large optical nonlinearities result from the gold film and nanoparticle arrays. The open-aperture (OA) curves shown in figures 3(a) and 4(a) reveal a normalized transmittance peak, indicating the presence of nonlinear absorption saturation in the gold film and nanoparticle array, while the peak-valley-shaped closed-aperture CA curves in figures 3(b) and 4(b) exhibit negative values for the nonlinear index n_2 in the two samples. Z-scan measurements for N2 and N4 give similar results as that of N3. The calculated values of $\chi^{(3)}$ as well as the FOM ($\chi^{(3)}/\alpha$) of the gold film and nanoparticle arrays are summarized in table 1. Considering the major uncertainty sources in the z-scan measurements, such as the laser intensity I, aperture diameter d, and film thickness L, etc, the total uncertainty of $\chi^{(3)}$ is estimated to be about 17–25%, as indicated in table 1. The measurements are repeated on different spots of the film/arrays in order to check the uniformity of the sample, and the results indicate that the relative uncertainty in $\chi^{(3)}$ is within the limits of 25%.

It is clear from table 1 that the $\chi^{(3)}$ values of well-ordered 2D nanoparticle arrays are much larger than that of the ultra-thin gold film consisting of randomly distributed spheroidal clusters. In order to investigate the effect of particle shape on the optical nonlinearities of materials, the values of $\chi^{(3)}$ were normalized by the absorption coefficient α, because the ultra-thin film/nanoparticle arrays contain different volume fractions of Au particles. It is worth noting that the FOM ($\chi^{(3)}/\alpha$) of the periodic nanoparticle arrays reached a value of 1.8×10^{-13} esu cm, which is about one order of magnitude larger than that of the ultra-thin gold film. It can be seen from figure 1(a) that the ultra-thin gold film in our experiments is a discontinuous film, with the absorption coefficient, $\alpha = 1.44 \times 10^5$ cm^{-1}, much smaller than that for a continuous Au film [14]. Either the nanoparticle arrays or the discontinuous thin film can be considered as a composite system with gold particles embedded in air matrix. The pronounced enhancement of the optical nonlinearities in the periodic nanoparticle arrays could be attributed to the stronger local field near the triangular nanoparticle surface. Both the theoretical and experimental studies demonstrated that the electromagnetic fields at the nanoparticle surface are more intense for nonhemispherical nanoparticles [15, 16]. In particular, the tips of a triangular particle with a very small radius of curvature tend to concentrate the electromagnetic field, and $|E|^2$ is as much as 12 000 times the incident field near the tips [16].

For a composite system, the FOM ($\chi^{(3)}/\alpha$) is expressed as follows [17]:

$$\frac{\chi^{(3)}_{\text{eff}}}{\alpha} = \frac{\lambda}{2\pi} \cdot \frac{f_i^2\sqrt{\varepsilon_d}}{\varepsilon''_m} \cdot \chi^{(3)}_m \tag{1}$$

where λ is the laser wavelength, ε_{d} is the dielectric constant of the host material, ε''_m is the imaginary part of the dielectric constant of the metal, $\chi^{(3)}_m$ is the third-order nonlinear susceptibility of the metal particle itself, and $f_i = E_i/E_0$ is defined as the local-field factor (E_i is the local field prevailing over the metal particles; E_0 is the incident field).

In the large particle limit (>20 nm), $\chi^{(3)}_m$ is almost independent of particle size. From equation (1) it is clear that the FOM strongly depends on the local-field factor. For spheroidal metal particles, the local-field factor f_i is expressed as [18]

$$f_i = \frac{3\varepsilon_d}{\varepsilon_m + 2\varepsilon_d} \tag{2}$$

where $\varepsilon_m = \varepsilon'_m + \text{i}\varepsilon''_m$ is the complex dielectric response of the metal particle. In the large particle limit, it is appropriate to calculate the ε_m value from the data for bulk Au [19]. Also, ε_{d} is the dielectric constant of the host material for air matrices $\varepsilon_{\text{d}} = 1$. Using equation (2), the value of $|f_i|$ is estimated to be 0.63 for spheroidal particles. But, in the case of nanoparticle arrays, we cannot calculate the local-field factor f_i of triangular-shaped nanoparticles from equation (2). However, we could estimate the f_i value from the measured linear absorption coefficient using the following equation [17]:

$$\alpha = p\frac{\omega}{nc}|f_i|^2\varepsilon''_m \tag{3}$$

where α is the absorption coefficient, ω is the angular frequency of the incident light, n is the refractive index of the matrix, c is the light velocity, and p is the volume fraction of metal particles; for the nanoparticle arrays in our experiment, $p = 0.08$. According to the α values listed in table 1, the local-field factor $|f_i|$ is estimated to be 1.7, which is about three times larger than that of spheroidal particles. So it is interesting to see that the enhancement of the FOM in the nanoparticle arrays is mainly due to the stronger local field near the triangular nanoparticles.

4. Conclusions

In summary, well-ordered two-dimensional gold nanoparticle arrays were fabricated using nanosphere lithography (NSL). The nonlinear optical properties of the nanoparticle arrays were investigated using the z-scan technique at 532 nm with 25 ps pulses. The FOM of the nanoparticle arrays is about one order of magnitude larger than that of the ultra-thin gold film consisting of randomly distributed spheroidal clusters. The enhancement of the optical nonlinearity could be due to the strong local field near the triangular nanoparticles. It is worth noting that, in well-ordered nanoparticle arrays, the homogeneity in size, shape, and distribution of the nanoparticles make it possible to get a better understanding of the origin of the enhancement of the nonlinearity, and then to further optimize the value of the FOM.

Acknowledgments

The authors gratefully acknowledge financial support from the National Natural Science Foundation of China, Grant 10574157, 90406024.

References

[1] Haché A and Bourgeois M 2000 *Appl. Phys. Lett.* **77** 4089
[2] Lepeshkin N N, Kim W, Safonov V P, Zhu J G, Armstrong R L, White C W, Zuhr R A and Shalaev V M 1999 *J. Nonlinear Opt. Phys. Mater.* **8** 191
[3] Hamanaka Y, Fukuta K, Nakamura A, Liz-Marzán L M and Mulvaney P 2004 *Appl. Phys. Lett.* **84** 4938
[4] Ballesteros J M, Solis J, Serna R and Afonso C N 1999 *Appl. Phys. Lett.* **74** 2791
[5] Lu S W, Sohling U, Mennig M and Schmidt H 2002 *Nanotechnology* **13** 669
[6] Haynes C L and Van Duyne R P 2001 *J. Phys. Chem.* B **105** 5599
[7] Yuen K P, Law M F, Yu K W and Sheng P 1997 *Phys. Rev.* E **56** 1322
[8] Huang J P and Yu K W 2005 *J. Opt. Soc. Am.* B **22** 1640
[9] Wen W J, Wang N, Ma H R, Lin Z F, Tam W Y, Chan C T and Sheng P 1999 *Phys. Rev. Lett.* **82** 4248
[10] Wen W J, Zheng D W and Tu K N 1998 *Phys. Rev.* E **57** 4516
[11] Guan DY, Chen Z H, Wang W T, Lu H B, Zhou Y L, Jin K J and Yang G Z 2005 *J. Opt. Soc. Am.* B **22** 1949
[12] Sheik-Bahae M, Said A A, Wei T H, Hagan D J and van Stryland E W 1990 *IEEE J. Quantum Electron.* **26** 760
[13] Izumi H, Ohata K, Hase T, Suzuki K, Morishita T and Tanaka S 1990 *J. Appl. Phys.* **68** 6331
[14] Smith D D, Yoon Y, Boyd R W, Campbell J K, Baker L A, Crooks R M and George M 1999 *J. Appl. Phys.* **86** 6200
[15] Jensen T R, Kelly K L, Lazarides A and Schatz G C 1999 *J. Cluster Sci.* **10** 295
[16] Haes A J, Zou S L, Schatz G C and Van Duyne R P 2004 *J. Phys. Chem.* B **108** 109
[17] Uchida K, Kaneko S, Omi S, Hata C, Tanji H, Asahara Y and Ikushima A J 1994 *J. Opt. Soc. Am.* B **11** 1236
[18] Böttcher C J F, Van Belle O C, Bordewijk P and Rip A 1973 *Theory of Electric Polarization* (Amsterdam: Elsevier Scientific)
[19] Palik E 1985 *Handbook of Optical Constants of Solids* (Orlando, FL: Academic)